RSC Advances

PAPER

View Article Online
View Journal | View Issue

Cite this: *RSC Adv.*, 2021, **11**, 32369

Preparation and characterization of self-healing furan-terminated polybutadiene (FTPB) based on Diels–Alder reaction

Min Xia, *[ab] Yanjie Zhang,[a] Qing Na,[a] Tao Guo,[a] Minghao Zhang,[a] Zhenyu Qi,[a] Ningning Liu,[c] Fanzhi Yang,[c] Yunjun Luo [ab] and Wei Yang*[a]

Received 24th June 2021
Accepted 13th September 2021

DOI: 10.1039/d1ra04732a

rsc.li/rsc-advances

Cracks generated in energetic composites will affect their mechanical properties and increase the risk of explosion when they are exposed to external stimuli. Therefore, self-healing properties of energetic composites have always been at the forefront of research in the field of high-performance energetic composites. Hydroxyl-terminated polybutadiene (HTPB) is a kind of binder widely used in propellants. A novel furan-terminated polybutadiene (FTPB) was synthesized by the reaction of NCO-terminated polybutadiene (IPDI-HTPB-IPDI) with furfuryl amine, and then self-healing binder films were obtained based on the DA adduct (FTPB-DA) through the reaction of furan with bismaleimide. The results show that FTPB-DA will transform into FTPB and BMI at 120 °C and recrosslinked at 60 °C to form FTPB-DA again, which gives it self-healing properties and the healing efficiency can reach 92.3%. Then, by adjusting the ratio of –NCO/–OH during the preparation process, we prepared self-healing binders with different DA adduct contents, and further studied the influence of DA adduct content on the mechanical properties and self-healing performance.

1. Introduction

Self-healing materials are a new type of smart material that can heal themselves when the material is damaged by simulating the self-healing mechanism of organisms. Self-healing materials can be divided into extrinsic healing materials and intrinsic healing materials according to whether additional healing agents are needed during the healing process.[1] The additives for extrinsic self-healing mainly include microcapsule,[2,3] micro-vascular[4,5] and hollow fiber.[6,7] Intrinsic self-healing is divided into dynamic covalent bonds and dynamic non-covalent bonds, among which dynamic covalent bonds include Diels–Alder,[8–10] disulfide bonds,[11,12] and acylhydrazone bonds;[13,14] and dynamic non-covalent bonds include hydrogen bonds,[15,16] metal ligand interactions,[17,18] and host–guest interactions.[19,20] Intrinsic self-healing enables the healing process to be carried out multiple times through the breaking and reorganization of dynamic covalent bonds or dynamic non-covalent bonds.

For energetic composites, a class of highly particle filled composite materials comprised of explosive crystals and a polymeric binder (*ca.* 5–10% by weight), there can be greater generation of cracks under external stimulation. Energetic composites are affected by external forces and heat during storage and transportation, which may produce micro-cracks and other damage. On one hand, the presence of micro-cracks will affect the mechanical properties of energetic composites. On the other hand, it may lead to hot spots in energetic composites, increasing the risk of explosion when they are subjected to external stimuli such as impact or friction. Introducing self-repairing properties into energetic composites can improve the stability and safety of the storage and transportation process, and prolong the service life.

Current research on self-healing energetic composites includes main two ways: the preparation of self-healing binders and improvement in the interface interaction of energetic composites.[21,22] Improving the interaction between the interfaces of energetic composites is mainly achieved by adding graphene to improve the thermal conductivity and adding surfactants to improve the bonding strength between composites.[23] Besides, the preparation of self-healing binders is more popular, mainly including self-healing binders based on disulfide bonds,[24,25] Diels–Alder,[26,27] and dynamic photocrosslinking reactions.[28] Energetic composites have poor UV light transmittance due to the presence of aluminum powder, so the application of dynamic photocrosslinking reactions in self-healing energetic composites is limited. Both disulfide bonds and DA adducts are thermally reversible dynamic covalent bonds, which have attracted the attention of researchers in the

[a]*School of Materials Science and Engineering, Beijing Institute of Technology, Beijing, 100081, China. E-mail: xmbit@bit.edu.cn*

[b]*Key Laboratory of High Energy Density Materials, Ministry of Education, Beijing 100081, China*

[c]*Frontier Interdisciplinary Research Institute, Beijing Institute of Technology, Beijing 100081, China*

study of self-healing binders. The preparation method of self-healing binders based on disulfide bonds and DA adducts is simple, and the healing efficiency is more than 90%.

HTPB is a binder widely used in composite solid propellants, so it is of great significance to study HTPB with self-healing properties. Liang[29,30] synthesized furan-terminated polybutadiene (FTPB) and trifurfuryl propane (TFP), and then designed HTPB-TDI (tolylene diisocyanate) and FTPB-PDMI (*N*,*N*′-(1,3-phenylene)bismaleimide) blending a self-healing system and the TFP chain-extending FTPB-PDMI self-healing system. While the process of synthesizing FTPB is relatively complicated, the mechanical properties of the binder film are poor (generally less than 2 MPa), and the self-healing efficiency can only reach 88%. In this study, a novel self-healing FTPB binder with simple preparation process and excellent mechanical properties was obtained. The FTPB is synthesized by the reaction of IPDI-HTPB-IPDI with furfuryl amine, and then crosslinked with BMI through a DA reaction. In addition, Liang's preparation method cannot control the content of DA adduct introduced into the system. Therefore, we prepared the FTPB with different furan contents by changing the –NCO/–OH ratio to obtain polyurethane crosslinked networks with different DA adduct contents, and further studied the effect of the content of DA adduct on the mechanical properties and self-healing properties of the FTPB binder film.

2. Experimental

2.1 Materials

Hydroxyl-terminated polybutadiene (HTPB, 50.8 mg per KOH per g, $f_n \approx 2.3$) was purchased from the Liming Research Institute of Chemical Industry and was used after 12 h of drying *in vacuo* at 60 °C. Furfuryl amine (FAm, 99%) and 1,1′-(methylenedi-1,4-phenylene) bismaleimide (BMI, 95%), isophorone diisocyanate (IPDI, 98%) were purchased from Aladdin Corporation of China and used as received. Dibutyltin dilaurate (DBTDL, 99%) was purchased from Shanghai Macleans Biochemical Technology Co., Ltd and used as received. Tetrahydrofuran (THF, 99%) was purchased from the Tianjin Jindong Tianzheng Fine Chemical Reagent Factory and used as received.

2.2 Synthesis of FTPB

The synthetic route of FTPB and FTPB-DA is shown in Scheme 1. FTPB was synthesized through a two-step conventional method. Firstly, IPD I (2 g) and HTPB (12 g) were charged into a 100 ml three-necked flask, followed by 10 ml of THF. The reaction proceeded with mechanical stirring under a nitrogen atmosphere at 80 °C for 3 h and then cooled in an ice-water bath. Secondly, furfuryl amine (0.874 g) dissolved in 2 ml of THF was added dropwise into the IPDI-HTPB-IPDI solution. Afterwards, the temperature was increased and kept at 80 °C for 2 h to ensure that all of the isocyanate was consumed by furfuryl amine, and a slightly yellow solid polymer was obtained as an intermediate product, named FTPB.

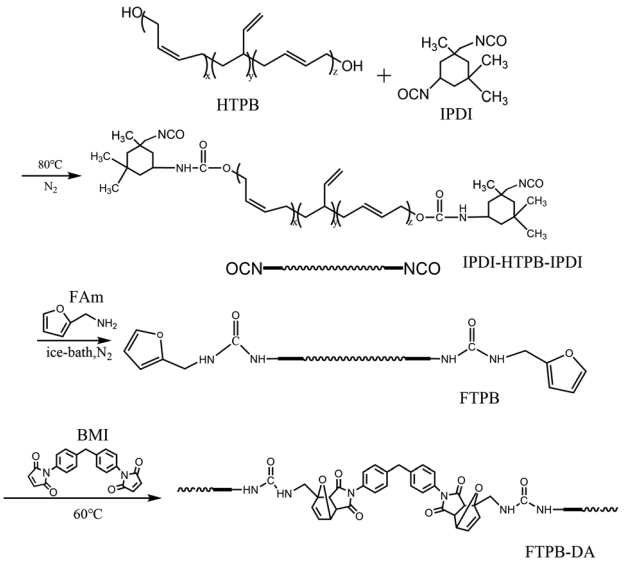

Scheme 1 Synthesis of FTPB and FTPB-DA.

2.3 Synthesis of FTPB-DA

BMI (1.612 g) dissolved in THF (20 ml) was added to the FTPB solution and the reaction was continued at 60 °C for 2 h. The final solution was poured into a polytetrafluoroethene (PTFE) plate and placed in a 60 °C oven for 48 h to obtain the final product (FTPB-DA2).

By adjusting the ratio of –NCO/–OH (molar ratio), FTPB with different furan contents can be prepared, and after further reaction with BMI, FTPB-DA with different DA adduct contents can be obtained. Therefore, we further synthesized samples of –NCO/–OH = 1.5 : 1, 2.5 : 1, and 3 : 1, and the samples were named FTPB-DA1.5, FTPB-DA2.5, and FTPB-DA3, where the synthesis method was the same as above.

2.4 Characterizations

Fourier transform infrared (FTIR) spectra were recorded with Nicolet 8700 infrared spectrometer from Thermo Nicolet Corporation (Waltham, MA, USA). FTIR spectra were recorded in the range of 700 to 3000 cm^{-1}. The nuclear magnetic resonance hydrogen spectrum (^{1}H-NMR) was performed on an Avance-400 spectrometer (Bruker, Switzerland) with deuterated $CDCl_3$ as the solvent at 25 °C.

Tensile performance was tested with an AGS-J electronic universal testing machine from Shimadzu Corporation (Kyoto, Japan), with a tensile rate of 100 mm min^{-1} at 25 °C, according to the GB/T528-1998 method to prepare the sample into a dumbbell-shaped spline. The self-healing efficiency was evaluated quantitatively with the recovery percent of tensile strength as in the following formula:

$$\eta = \sigma_{healed}/\sigma_{original} \times 100\%$$

where σ_{healed} and $\sigma_{original}$ are the tensile strength of the healed sample and the original sample, respectively.

Polarizing optical microscopy (POM) analysis was performed with a DM2500P polarized microscope from Leica Corporation (Wetzlar, Hesse, German) using a 12 V 100 W halogen lamp. The thermal reversibility of FTPB-DA was studied by DSC1/500/578 from Mettler-Toledo (USA) from 25 to 150 °C at a heating rate of 10 K min^{-1} under nitrogen flow. The thermal stability was measured with a TGA/DSC1 SF/417-2 from Mettler-Toledo (USA) at a heating rate of 10 K min^{-1} from 30 °C to 600 °C.

3. Results and discussion

3.1 Structural characterization of FTPB and FTPB-DA

First, the molecular structures of FTPB and FTPB-DA were characterized by FTIR spectra, and the results are shown in Fig. 1. In the FTIR spectra of FTPB, the peaks at 1148 cm^{-1} and 995 cm^{-1} are the respiratory vibration peaks of the furan ring. In addition, the characteristic peak of –NCO at 2270 cm^{-1} has basically disappeared, and the bending vibration peak of –C–N in the urea group appears at 1560 cm^{-1}, indicating that the furan ring has been introduced into the molecular chain by the reaction of furfuryl amine with IPDI-HTPB-IPDI. In the FTIR spectra of FTPB-DA, the respiratory vibration peak of the C=C in the DA adduct appears at 1777 cm^{-1}, and the respiratory vibration peak of the C–C in the DA adduct appears at 1189 cm^{-1}. The appearance of the new characteristic peak indicates that the DA adduct has been successfully introduced into the FTPB binder.

^{1}H-NMR spectra of FTPB and FTPB-DA confirmed the FTIR result, as shown in Fig. 2. The peaks at $\delta = 7.55$ ppm (–O–CH=CH–, a), 6.31 ppm (–CH=, b) and 6.22 ppm (–CH=, c) confirm the successful synthesis of FTPB. The reaction of FTPB with BMI was investigated *via* the testing of the 1H-NMR spectra of the reaction solution after 30 min at 60 °C. Compared with the 1H-NMR spectra of FTPB, the characteristic peaks of the furan ring at $\delta = 7.55$ ppm (a), 6.31 ppm (b) and 6.22 ppm (c) are significantly weaker. In addition, some new peaks appeared at $\delta =$ 6.53 ppm, 6.62 (b′ and c′), 5.31 ppm (a′), 3.18 ppm (e), and 3.22 ppm (f). The variation in each characteristic peak is consistent with Du,[31] which indicates that the DA reaction has been successfully carried out.

3.2 Self-healing properties

3.2.1 Polarizing Optical Microscopy (POM) analysis. The FTPB-DA films were prefabricated with scratches of a depth of 0.5 mm, and the films were heated at 120 °C. With FTPB-DA2 as an example, the morphological change in the crack during the healing process was observed under a polarizing optical microscope. As shown in Fig. 3, the crack interface gradually blurred after heating at 120 °C for 5 min, and the crack disappeared in about 10 min. FTPB-DA transformed into FTPB and BMI through the reverse DA (r-DA) reaction at 120 °C. Small molecules diffuse into the crack through thermal movement to fill the crack, so the crack morphology gradually approaches the original sample. In addition, the cross-linking points were unwound as a result of r-DA reaction, so the surface of the FTPB-DA film became sticky. After heating at 60 °C, FTPB and BMI react to form DA adducts to restore mechanical properties. The thermoreversible self-healing process of FTPB-DA shown in Scheme 2. In order to further quantitatively analyze the self-healing performance, tensile testing was performed.

3.2.2 Mechanical healing efficiency. The mechanical properties of films with different –NCO/–OH ratios were studied

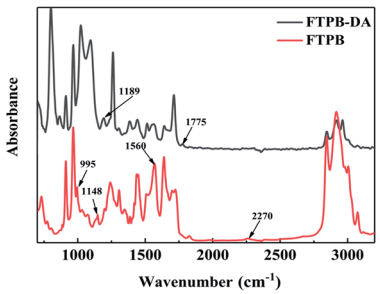

Fig. 1 FTIR spectra of FTPB and FTPB-DA.

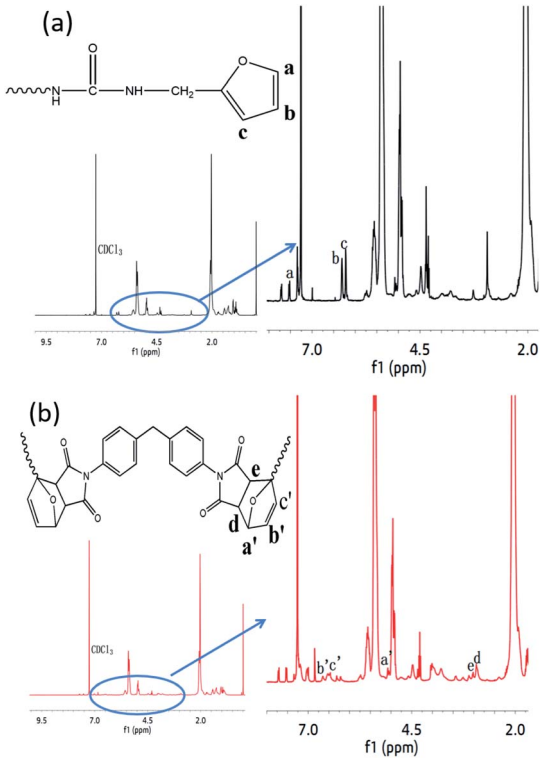

Fig. 2 (a) ^{1}H-NMR spectra of FTPB (b) ^{1}H-NMR spectra FTPB-DA.

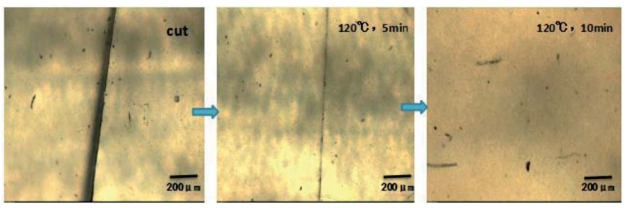

Fig. 3 POM images of a crack in FTPB-DA2 during the healing process.

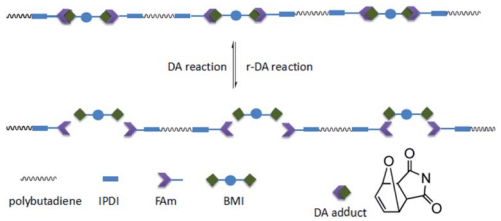

Scheme 2 Thermoreversible self-healing process of FTPB-DA.

by tensile testing. In the tensile testing, no fewer than 5 samples (5–7) were selected for each –NCO/–OH ratio, and finally the stress–strain curve was selected whose breaking strength was closest to the average. The difference in breaking strength of samples with the same ratio is less than 0.1 MPa. As shown in Fig. 4, the modulus of the film increases as the –NCO/–OH ratio increases, while the elongation follows the opposite trend. This is because the content of hard segments increases with the increase in –NCO/–OH ratio, and at the same time furan and maleimide react to form more DA adducts. The two benzene rings in BMI and the six-membered ring of the DA adduct are rigid structures. The rigid structure has a large steric hindrance, which can prevent the intermolecular chain from sliding, so the modulus of the film gradually increases with the –NCO/–OH ratio, while the elongation does the opposite. However, the FTPB-DA film with an –NCO/–OH ratio of 2 : 1 had the highest tensile strength. This is because when the –NCO/–OH ratio is greater than 2, the film is hardened due to the high hard segment content, which causes the tensile strength to decrease; even when the –NCO/–OH ratio is 3, the film appears to show yielding behavior.

The self-healing films were pre-cracked: a crack with a width of 5 mm and a depth of 5 mm was drawn within 30 seconds with a sharp knife. The pre-cracked films were heated at 120 °C for 20 minutes and then heated at 60 °C for 24 hours to heal the cracks. The stress–strain curves of the original sample, the cut sample and the healed sample are shown in Fig. 5, where it can be seen that all samples have self-healing ability. The self-healing efficiency was calculated and is listed in Table 1. FTPB-DA2 has the highest self-healing efficiency, which can reach 92.33%. The content of DA adduct of FTPB-DA1.5 involved in the self-healing process is insufficient, so the healing efficiency is relatively low. FTPB-DA2.5 and FTPB-DA3 have more DA bonds than FTPB-DA2, but the self-healing efficiency has not been further improved. The self-healing efficiency of FTPB-DA2.5 is 86.61%, and the self-healing efficiency of DA-3 is only 63.58%. This is because the high content of hard segments restricts the movement of FTPB and BMI. When heated at 120 °C, the activity of small molecule movement is low, which leads to a poor filling effect on the crack surface. In addition, when heated at 60 °C, the low molecular movement activity leads to low probability of contact between FTPB and BMI, so the formation efficiency of DA adducts is also low. Therefore, the healing process in the FTPB-DA system not only requires a sufficient number of DA adducts, but the movement activity of the molecular chain also has an important impact on the healing process.

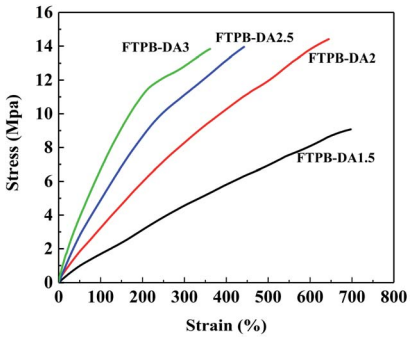

Fig. 4 Comparison of the mechanical properties of FTPB-DA with different –NCO/–OH ratio.

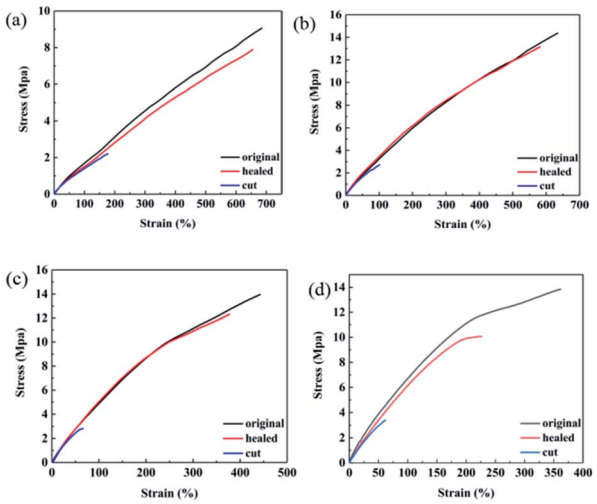

Fig. 5 Stress–strain curves of samples with different –NCO/–OH ratios.

3.3 Thermal reversibility

3.3.1 DSC. DSC measurement is an efficient method to study the thermal reversibility of the synthesized polymer. The film prepared based on the DA reaction was named DA0, and it was subjected to the heat treatment shown in Scheme 3 for a DSC test.

Table 1 Self-healing efficiency of samples under different –NCO/–OH ratio

	Strength (MPa)		
FTPB-DA	Original	Healed	η (%)
$R = 1.5$	9	7.8	86.78
$R = 2$	14.35	13.25	92.33
$R = 2.5$	13.82	11.97	86.61
$R = 3$	13.51	8.59	63.58

The DSC curves are shown in Fig. 6. FTPB did not show an endothermic peak during the heating process, while the DA0 sample exhibits a significant endothermic peak around 120 °C, indicating that the DA0 sample undergoes the r-DA reaction and absorbs a large amount of heat when the temperature rises to 120 °C. A higher r-DA reaction temperature is detrimental to the safety of energetic composites. From the DSC curve, it can be seen that the r-DA reaction of DA0 starts at 100 °C, but the r-DA reaction will take a long time at a low temperature. In order to facilitate the study of self-healing properties, 120 °C was used for the r-DA reaction in this paper. The rDA1 sample was obtained by heating the DA0 sample at 120 °C for 15 minutes. The endothermic peak of the DSC curve of rDA1 disappeared, indicating that the DA0 sample had undergone the r-DA reaction after high-temperature treatment, so there were no DA adducts in the rDA1 sample. The DA1 sample was obtained by heating the rDA1 sample at 60 °C for 24 h. The DSC curve of rDA1 showed the endothermic peak of the r-DA reaction at 135 °C. The change in DSC curves proves that there is a thermally reversible DA reaction in FTPB-DA. The rise in the r-DA reaction temperature is because maleimide will self-polymerize to form irreversible bonds at high temperature,[32] so the duration of high-temperature treatment should be controlled during the self-healing process.

3.3.2 DMA. Dynamic mechanical analysis (DMA) was conducted to gain an understanding of the viscoelastic behavior of FTPB-DA at different temperatures. Fig. 7a shows the storage modulus (E_1) as a function of temperature for different samples where a two-stage decrease can be observed. The first drop in E_1 can be attributed to the glass transition of the soft segment in FTPB-DA at a low temperature of around −80 °C. The second drop in E_1 can be attributed to the dissociation of DA adduct. When the temperature rises to 100 °C, FTPB-DA undergoes the r-DA reaction to transform into FTPB and BMI, resulting in a rapid decrease in the curve of E_1, which characterizes the elasticity of the sample. In the second drop stage for E_1, it can be seen that the moduli of FTPB-DA1.5 and FTPB-DA2 decline faster, indicating that the kinetic activities of the FTPB-DA1.5 and FTPB-DA2 molecular chains are higher than those of FTPB-DA2.5 and FTPB-DA3 at high temperature. Therefore, the molecular chain can spread to the crack section faster and fill the crack more quickly, which is beneficial to the self-healing performance.

As shown in Fig. 7b, there are two peaks in the tan δ curve of each sample and the peak temperature of tan δ is listed in Table 2. The first peak temperature corresponds to the glass transition temperature (T_g) of the polymer. The contents of hard segment in each FTPB-DA film are 18.6%, 27.36%, 34.17%, and 39.92%, respectively. It can be seen from Table 2 that as the content of the hard segment increases, the T_g of the soft segment of FTPB-DA is gradually elevated. The T_g of the soft phase region will be raised only when a significant number of hard segments are mixed with soft segments.[33] The difference in T_g indicates that some soft segments dissolve with hard segments in FTPB-DA, and the hard segments have an obstruction effect on the movement of soft segments. Therefore, the healing efficiency of the samples does not always increase with an increase in the DA adduct content, which is consistent with the mechanical test results. The second peak of the tan δ curve at 120 °C is attributed to the dissociation peak of FTPB-DA. The second peak of the tan δ curve further indicates that FTPB-DA will undergo an r-DA reaction during the self-healing process. The temperature of the dissociation peak gradually increases with an increase in the –NCO/–OH ratio. The meaning of tan δ is the energy lost by friction between chain segments. After the r-DA reaction, the samples with a higher content of hard segments give the molecular chains sufficient kinetic activity at higher temperature, so the dissociation peak will appear at a higher temperature.

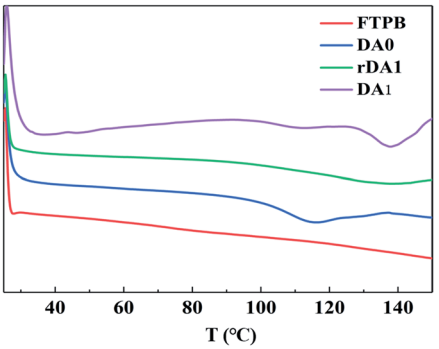

Fig. 6 DSC curves of FTPB-DA after different heat treatment.

3.4 Thermal stability

With FTPB-DA2 as an example, the thermal stabilities of FTPB and FTPB-DA2 were tested by TGA. As shown in Fig. 8, FTPB and FTPB-DA2 have no obvious quality loss before 200 °C, indicating that both have high thermal stability. The thermal decomposition of FTPB and FTPB-DA2 can be divided into two stages. When the temperature rises to 250 °C, the thermal stability of the urea bond and carbamate bond is prone to thermal decomposition due to the weak bond energy. So the weight loss in the first stage is attributed to the decomposition of

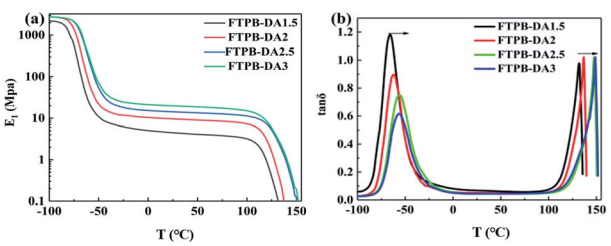

Fig. 7 DMA curve of FTPB-DA with different –NCO/–OH ratios: (a) storage modulus curve; (b) loss factor curve.

DA0 —120°C 15min→ rDA1 —60°C 24h→ DA1

Scheme 3 The heat treatment of DSC samples.

Table 2 The peak temperature of tan δ

Sample	Peak 1 (°C)	Peak 2 (°C)
FTPB-DA1.5	−65.5	131.9
FTPB-DA2	−61.8	136.7
FTPB-DA2.5	−56.3	147.7
FTPB-DA3	−56.3	148.7

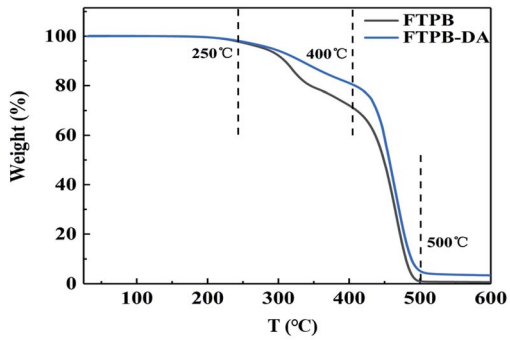

Fig. 8 The TGA curves of FTPB and FTPB-DA.

carbamate and urea groups in the main chain. The second stage of decomposition starting at 400 °C is attributed to the thermal decomposition of the soft segment of FTPB. FTPB has almost completely decomposed at 500 °C, while FTPB-DA still has 3.5% char residue. FTPB-DA can be converted into FTPB and BMI through an r-DA reaction at high temperature. The two benzene rings in BMI are rigid structures with good thermal stability and high char residue content, which also proved that BMI was successfully introduced into FTPB-DA.

4. Conclusion

We first synthesized furan-terminated polybutadiene (FTPB) through a two-step method, and then obtained a self-healing binder film based on the DA adduct (FTPB-DA) through the reaction of furan and bismaleimide. The structures of FTPB, FTPB-DA were confirmed by FTIR and 1H-NMR, showing that the DA adduct was successfully introduced into the polymer. According to the results obtained by DSC and DMA, FTPB-DA exhibited good thermal reversibility. FTPB-DA transformed into FTPB and BMI at 120 °C and recrosslinked at 60 °C to form FTPB-DA again. POM analysis and tensile tests show that FTPB-DA has excellent self-healing performance. When the damaged FTPB-DA2 is heated at 120 °C for 20 min and 60 °C for 24 h, the healing efficiency can reach 92.33%. The self-healing performance of FTPB-DA samples with different contents of DA adduct were evaluated, and the results prove that the self-healing process is the result of the combined effect of the thermally reversible DA reaction and the thermal movement of the molecular chain. Therefore, the self-healing efficiency of binder film can be adjusted by controlling the content of DA adduct.

Conflicts of interest

The authors declare that they have no known competing financial interests or personal relationships that could have appeared to influence the work reported in this paper.

Notes and references

1 R. S. Trask, H. R. Williams and I. P. Bond, *Bioinspiration Biomimetics*, 2007, **2**, 1.
2 S. R. White, N. R. Sottos and P. H. Geubelle, *Nature*, 2001, **409**, 794–797.
3 W. Du, J. Yu, Y. Gu, Y. Li, X. Han and Q. Liu, *Constr. Build. Mater.*, 2019, **202**, 762–769.
4 K. S. Toohey, N. R. Sottos, J. A. Lewis, J. S. Moore and S. R. White, *Nat. Mater.*, 2007, **6**, 581–585.
5 S. R. Kim, B. A. Getache and J. H. Kim, *J. Membr. Sci.*, 2017, 531.
6 C. Dry, *Compos. Struct.*, 1996, **35**, 263–269.
7 S. Kling and T. Czigany, *Compos. Sci. Technol.*, 2014, **99**, 82–88.
8 P. Du, M. Wu, X. Liu, Z. Zhen and Y. Zhang, *J. Appl. Polym. Sci.*, 2014, **131**, 40234.
9 P. Tanasi, M. H. Santana and R. Verdejo, *Polymer*, 2019, **175**, 15–24.
10 C. C. Lin, D. K. Sheng and X. D. Liu, *Polymer*, 2018, **140**, 150–157.
11 Y. Amamoto, H. Otsuka, A. Takahara and K. Matyjaszewski, *Adv. Mater.*, 2012, **24**, 3975–3980.
12 Y. Xu and D. A. Chen, *Macromol. Chem. Phys.*, 2016, **217**, 1191–1196.
13 D. D. Zhang, Y. B. Ruan, B. Q. Qiao, X. Deng, G. H. Chen and Y. M. Liu, *Polymer*, 2017, **120**, 189–196.
14 N. Kuhl, S. Bode, R. K. Bose, J. Vitz, A. Seifert and S. Hoeppener, *Adv. Funct. Mater.*, 2015, **25**, 3295–3301.
15 F. Sordo, S. J. Mougnier, N. Loureiro, F. Tournilhac and F. Michaud, *Macromolecules*, 2015, **48**, 4394–4402.
16 H. Zhang, H. Xia and Y. Zhao, *ACS Macro Lett.*, 2012, **1**, 1233–1236.
17 Y. Shi, M. Wang, C. Ma, Y. Wang, X. Li and G. Yu, *Nano Lett.*, 2015, **15**, 6276–6281.
18 I. Hussain, S. M. Sayed, S. Liu, F. Yao, O. Oderinde and G. Fu, *Adv. Funct. Mater.*, 2018, **100**, 219–227.
19 M. Zhang, D. Xu, X. Yan, J. Chen and F. Huang, *Angew. Chem., Int. Ed.*, 2012, **51**, 7011–7015.
20 J. B. Hou, X. Q. Zhang, D. Wu, J. F. Feng, D. Ke and B. J. Li, *ACS Appl. Mater. Interfaces*, 2019, **11**, 12105–12113.
21 Y. J. Zhang, M. Xia, W. Yang, F. Z. Yang and Y. J. Luo, *Chin. J. Chem.*, 2020, **38**, 1807–1816.
22 M. Xia, Y. J. Zhang, S. J. Ding and Y. J. Luo, *Chin. J. Explos. Propellants*, 2019, **42**, 531–539.
23 X. Huang, Z. Huang, J. C. Lai, L. Li, G. C. Yang and C. H. Li, *Compos. Sci. Technol.*, 2018, **167**, 346–354.
24 Y. Li, Z. Yang, L. Ding, L. Pan, J. Zhang, X. Zheng and C. Lin, *React. Funct. Polym.*, 2019, **144**, 104342.
25 X. Zhai, Y. Sonng, M. Zhao, Y. Liang, W. Zhou and L. Xiao, *Chin. J. Energetic Mater.*, 2019, **27**, 131–136.

26 Y. Li, Z. Yang, J. Zhang, L. Ding, L. Pan, C. Huang, X. Zheng, C. Zeng and C. Lin, *Polym. Test.*, 2019, **76**, 82–89.
27 C. Y. Liang, J. Li, M. Xia, G. P. Li and Y. J. Luo, *Polymers*, 2017, **9**, 200.
28 R. Yan, MASc, Beijing Institute of Technology, Beijing, 2019Thesis.
29 C. Y. Liang, J. Li, M. Xia, G. P. Li and Y. J. Luo, *Polym. Mater. Sci. Eng.*, 2018, **34**, 12–16.
30 C. Y. Liang, MASc, Beijing Institute of Technology, Beijing, 2017Thesis.
31 P. Du, M. Wu, X. Liu, Z. Zhen and Y. Zhang, *New J. Chem.*, 2014, **38**, 770–776.
32 Y. L. Liu and C. Y. Hsieh, *J. Polym. Sci., Part A: Polym. Chem.*, 2006, **44**, 905–913.
33 W. B. Ying, Z. Yu, D. H. Kim, K. J. Lee and R. W. Li, *ACS Appl. Mater. Interfaces*, 2020, **12**, 11072–11083.